

Article

The Photosynthesis of *Populus euphratica* Oliv. Is Not Limited by Drought Stress in the Hyper-Arid Zone of Northwest China

Guanlong Gao ^{1,2,3,4}, Qi Feng ² , Xiande Liu ³, Tengfei Yu ²  and Rongxin Wang ^{3,*}

¹ College of Environment and Resource, Shanxi University, Taiyuan 030006, China

² Northwest Institute of Eco-Environment and Resources, Chinese Academy of Sciences, Lanzhou 730000, China

³ Academy of Water Resources Conservation Forests in Qilian Mountains of Gansu Province, Zhangye 734000, China

⁴ Shanxi Laboratory for Yellow River, Taiyuan 030006, China

* Correspondence: zywangrx@163.com

Abstract: The Ejina Oasis is located in the lower reaches of the Heihe River Basin of northwestern China. It is one of the most arid regions in the world, and *Populus euphratica* Oliv. is the foundation species of the desert riparian forests there. The photosynthesis of *P. euphratica* is one of the first physiological processes that is most likely to be affected by the extremely arid climate conditions. The factors impacting photosynthesis can be divided into stomatal and non-stomatal limitations. In order to investigate whether the photosynthesis of *P. euphratica* was limited and, if so, whether this limitation was caused by drought stress in the *P. euphratica* Forest Reserve on the Ejina River, we analyzed stomatal, non-stomatal, and relative stomatal limitations (reflecting the relative importance of the stoma in controlling the processes of photosynthesis) of photosynthesis. The results show that, at the beginning of the midday depression of photosynthesis, the values of stomatal limitation of photosynthesis (L_s) peaked, with its predominance being supported by sub-stomatal CO_2 concentrations (C_i) being at a minimum. Thereafter, L_s decreased and non-stomatal limitation ($C_i/\text{stomatal conductance}$ (g_s)) increased sharply, indicating that the non-stomatal limitation of photosynthesis was predominant. Both L_s and relative stomatal limitation of photosynthesis increased in the morning, and then decreased, whereas C_i/g_s showed the opposite trend. We concluded that *P. euphratica* did not experience drought stress by analyzing leaf water potential, groundwater table, and the decoupling coefficient (a parameter characterizing the coupling degree between vegetation canopy and atmospheric water vapor flux); however, the L_s values of *P. euphratica* were much greater than those of other species. This was likely because *P. euphratica* has a relatively conservative water use strategy even when growing under favorable water conditions. Extremely high temperatures caused the closure of the stoma to reduce transpiration, resulting in more intense stomatal limitations of photosynthesis.

Keywords: photosynthesis; stomatal limitation; non-stomatal limitation; relative stomatal limitation



Citation: Gao, G.; Feng, Q.; Liu, X.; Yu, T.; Wang, R. The Photosynthesis of *Populus euphratica* Oliv. Is Not Limited by Drought Stress in the Hyper-Arid Zone of Northwest China. *Forests* **2022**, *13*, 2096. <https://doi.org/10.3390/f13122096>

Academic Editor: Giovanbattista De Dato

Received: 1 November 2022

Accepted: 6 December 2022

Published: 8 December 2022

Publisher's Note: MDPI stays neutral with regard to jurisdictional claims in published maps and institutional affiliations.



Copyright: © 2022 by the authors. Licensee MDPI, Basel, Switzerland. This article is an open access article distributed under the terms and conditions of the Creative Commons Attribution (CC BY) license (<https://creativecommons.org/licenses/by/4.0/>).

1. Introduction

Water deficit constitutes one of the most critical challenges for species and ecosystems [1], and is an important environmental factor inhibiting the growth and reducing the yield of plants worldwide [2,3]. Low water availability reduces the plant carbon balance [4] and limits plant growth through its negative effects on photosynthesis [5]. Previous studies have shown that photosynthesis is one of the first physiological processes to be affected by drought stress [6]. Farquhar and Sharkey [7] note that the limitations of photosynthesis consist of two different processes: (1) stomatal limitation of photosynthesis, wherein the intercellular CO_2 concentration (C_i) cannot meet the needs of photosynthesis owing to the limitation of stomatal conductance (g_s); and (2) non-stomatal limitation of photosynthesis,

wherein the chloroplast and Rubisco activities and ribulose biphosphate (RuBP) regeneration are decreased. Jones [8] proposed relative stomatal limitation of photosynthesis to quantify the relative importance of the stoma in controlling the processes of photosynthesis. Theoretically, stomatal closure can be adopted as an adaption to save water under drought stress conditions; values of g_s will decrease to reduce water loss through transpiration, and plants will become relatively conservative water users with stomatal limitation of photosynthesis as the dominant mechanism. Previous studies have supported this viewpoint, and have also shown that non-stomatal limitation of photosynthesis will predominate as drought stress intensifies [9–12].

Dryland biomes cover approximately 41.5% of Earth's land surface [13] and are expanding globally [14]. Arid regions are expected to become drier as a result of climate change [15–17]. Dryland ecosystems represent a dynamic, but poorly understood component of the global carbon, water, and energy cycles [18]. In such regions, drought stress may modify the morphological (leaf size, length, width and mass per area) and physiological characteristics (maximum photosynthesis rate, electron transfer rate, stomatal conductance, leaf water potential and transpiration) of plants [19]. The Ejina Oasis, located in the lower reaches of the Heihe River Basin of northwestern China, is one of the most arid regions in the world [20]. Annual rainfall is less than 50 mm [21], and little water is released from the upper and middle reaches of the river basin. Within this water-limited environment, the riparian zone represents a distinct ecotone between rivers and the surrounding drylands, and is of considerable ecological importance [22]. *Populus euphratica* Oliv. is a rare, ancient, and endangered tree species only presents in inland river basins located in the desert and semiarid areas of Central Asia. It is a typical phreatophyte, and is also the foundation species of the desert riparian forest in the lower Heihe River Basin. Its regular growth is important for protecting the basin ecosystem and biodiversity, preventing desertification, and forming a natural barrier to support the existence of the Ejina Oasis. Because of the populace's excessive use of water resources, the *P. euphratica* forests in this region have degenerated in the past century [23]. The Ecological Water Diversion Project was initiated in 2000 [24,25] to restore these riparian forests, which aimed to increase runoff to 0.95 billion m^3 /year [26]. Although the lower Heihe River Basin actually receives an average of 1.12 billion m^3 /year of runoff, the recovery of *P. euphratica* has not been satisfactory [27,28]. Consequently, we hypothesized that current water resources remain insufficient to maintain regular physiological processes, such as photosynthesis, that affect the growth of *P. euphratica*.

The objective of our research was to identify if the photosynthesis of a desert riparian *P. euphratica* forest was limited, and if so, whether this limitation was caused by drought stress. To this end, we analyzed stomatal, non-stomatal, and relative stomatal limitations of photosynthesis as well as other related physiological parameters. In recent years, the photosynthesis of *P. euphratica* has been studied by Chen et al. [29], Wang et al. [30] and Zhou et al. [31] in the lower reaches of the Tarim River, and Zheng et al. [32] in the nursery, while few studies have been conducted in the lower reaches of the Heihe River, especially after the implementation of the Ecological Water Diversion Project. Zhu et al. [33] studied the effects of seasonal fluctuations of temperature on the photosynthesis of *P. euphratica* in the lower reaches of the Heihe River; however, a comprehensive analysis of the types of photosynthetic limitations is urgently needed. Moreover, most research has focused on analyzing water potential (ψ_L , MPa) [23,34] or depth to the groundwater table (GWT, m) [34,35] to determine drought stress. Using ψ_L and GWT depth, we also analyzed the decoupling coefficient (Ω , $0 \leq \Omega \leq 1$), which indirectly reflects the water supply conditions of vegetation [36–38].

2. Materials and Methods

2.1. Experimental Site

We recorded measurements of leaf gas exchange in *P. euphratica* leaves in the *P. euphratica* Forest Reserve on the Ejina River (Inner Mongolia, China) from June to Septem-

ber, which is the main growing season of *P. euphratica* based on phenology according to Abdurahman et al. [39] in 2013 and 2014 (Figure 1, 42°21' N, 101°15' E, altitude 920.5 m a.s.l.). In the forest reserve, the average tree age is 39 years, with good growth status. The trees have an average height of 10.2 m, an average diameter at breast height of 24.67 cm, and an average crown breadth of 442 cm × 450 cm. The soil is approximately 2 m deep sandy loam and has a volumetric water content of 0.35 m³ m⁻³. The bulk density of the soil is 1.53 g cm⁻³.

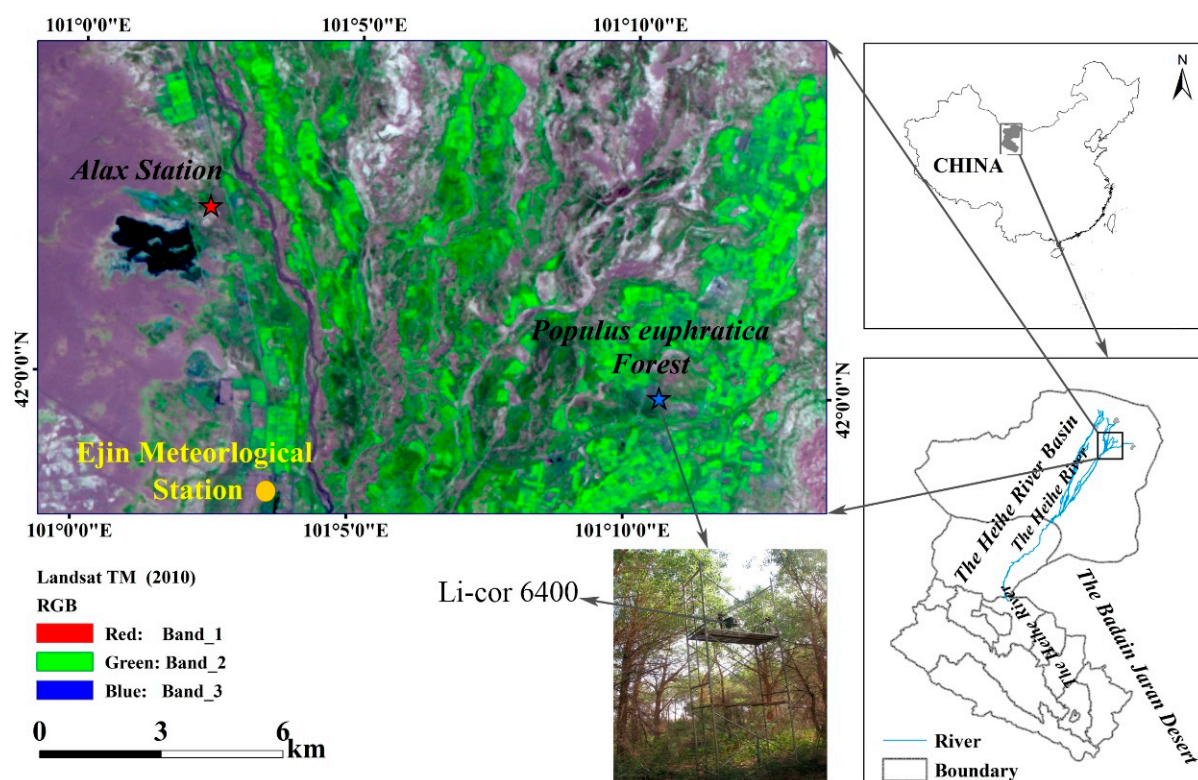


Figure 1. Map of the study area.

2.2. Sap Flow and Transpiration

We estimated the sap flow velocity (V_s , cm h⁻¹) by scaling up the sapwood area (A_s , cm²) from the tree to the stand based on the relationship between A_s and diameter at breast height (DBH, cm) for *P. euphratica* trees [20]. We selected three trees that were representative of the surrounding stand; the selected trees did not significantly differ in height, DBH, or A_s according to the stand means (*t*-test) (Table 1). We measured V_s using the heat ratio method (SFM1, ICT Inc., Armidale, Australia) by inserting two sensors into the xylem tissue of the trunks at DBH height. Because the thickness of the sapwood was less than the length of the probe, the outer (22.5 mm depth) V_s was selected for analysis. Data from the inner (7.5 mm depth) probe were always low and smooth, and even negative (data not shown), suggesting that it was inserted into heartwood, and the data were discarded. After insertion, the exposed cambium was covered with aluminum foil to reduce the effects of ambient temperature fluctuation and direct solar radiation. All probes were connected to an AM416 multiplexer (Campbell Scientific Inc., Logan, UT, USA) powered by 12 V car batteries. The heater was set up to send a pulse every 30 min, and temperature ratios were recorded continuously with a data logger (CR10x, Campbell Scientific Inc., Logan, UT, USA) connected to the multiplexer by four shielded conductor cables. Then, using the methods of Jarvis and McNaughton [40], we recorded heat pulse velocity (V_h , cm h⁻¹), made corrections related to probe wounds and misalignment, and calculated hourly whole-tree sap flow (F_s , L h⁻¹) as the product of A_s and V_s of the outer measurement point [22].

Total daily transpiration (T , mm d⁻¹) during the study periods was calculated by dividing the 24 h cumulative sum of F_s by the stand area.

Table 1. Summary of biological parameters for the three selected *Populus euphratica* trees.

Tree Number	Height (m)	DBH (cm)	A_s (cm ²)
1	10.6	23.9	225.6
2	10.4	21.7	206.4
3	10.3	30.4	361.2
Sig. (2-tailed)	0.105	0.623	0.718

Difference was tested by the *t*-test at a significance level of $p = 0.05$. DBH diameter at breast height, A_s sapwood area.

2.3. Leaf Gas-Exchange and Water Potential

We selected six trees each year to measure leaf gas exchange, on four or five sunny days every month (for a total of 18 days in 2013 and 19 days in 2014). Based on an LI-6400 portable photosynthesis system (LI-COR Inc., Lincoln, NE, USA), we measured all available parameters under ambient conditions using a natural light source, including net photosynthesis (P_n , $\mu\text{mol CO}_2 \text{ m}^{-2} \text{ s}^{-1}$), stomatal conductance (g_s , $\text{mol H}_2\text{O m}^{-2} \text{ s}^{-1}$), sub-stomatal and ambient CO_2 concentrations (C_i and C_a , $\mu\text{mol CO}_2 \text{ mol}^{-1}$), photosynthetically active radiation (PAR, $\mu\text{mol m}^{-2} \text{ s}^{-1}$), and vapor pressure deficit (VPD, kPa). We took hourly measurements in three fully expanded leaves of each tree from the east and west, and recorded three replications for each leaf. Eventually, the hourly value of each parameter was averaged from 54 sets of data. We conducted the measurements between 8:00 and 20:00, advancing or postponing the observation sessions by 1 h depending on the specific timing of sunrise and sunset. We used a sky lift to reach the canopy when measuring the leaves (Figure 1).

Using a plant pressure chamber (1505D, PMS Instrument Co., Albany, OR, USA), we measured hourly diurnal variation in ψ_L in three fully expanded and mature leaves, from each tree, ensuring the west, south, and east of the crown were exposed to direct solar radiation. The hourly value of ψ_L was averaged from 18 sets of data. We wrapped the samples in a sealed plastic bag, using a moist paper towel to prevent sudden dehydration under high-temperature conditions before cutting from the petiole with a razor blade. We measured ψ_L within a minute after detaching the leaves.

2.4. Meteorological and Hydrologic Parameters

We recorded meteorological variables, including air temperature (T_a , °C), relative humidity (h_s , %), net radiation (R_n , W m^{-2}), and wind speed (u , m s^{-1}), at a height of 20 m using a CR3000 datalogger at 0.5 h intervals. We measured R_n using a four-component net radiometer (model CNR-4, Kipp & Zonen, The Netherlands), and T_a and h_s using temperature/relative humidity sensors (model HMP45C, Campbell Scientific, USA). To measure GWT depth automatically, one well was drilled to about 6 m in depth, and a pressure transducer (HOBO-U20, Onset Computer Corporation, Bourne, MA, USA) was installed to monitor the changes in the submerged pressure (P_{sub} , kPa) at 0.5 h intervals. The barometric pressure was subtracted from P_{sub} to obtain the pressure that was exerted only by the water column above the sensors. Water head data were then converted to GWT values, using the measured distance between sensors and ground surface at the well.

2.5. Data Analysis

The observational days for measuring leaf gas-exchange parameters were selected for analysis. All the data collected on these days, including those manually measured and those automatically recorded, were processed at 1 h intervals, except those for the GWT depth (which is given in daily values for 2014). Then, we calculated the averaged values of each parameter at the same hour on different observational days each month to analyze

the variation trends. We used SPSS 19.0, Origin 8.0, and SigmaPlot 13.0 for all statistical analyses and plotting.

2.6. Formulae

2.6.1. Stomatal, Non-Stomatal, and Relative Stomatal Limitations of Photosynthesis and Related Parameters

Stomatal limitation of photosynthesis, L_s , can be calculated according to the following formula described by Berry and Downton [41]:

$$L_s = 1 - C_i / (C_a - \Gamma), \quad (1)$$

where Γ is the CO_2 compensation point of assimilation in the presence of dark respiration. Γ can always be neglected as its value is always much smaller than that of C_a and C_i [42–44]. The formula can be expressed as:

$$L_s = 1 - C_i / C_a, \quad (2)$$

Kicheva et al. [45] took the occurrence of high C_i values at reduced g_s as an indication of non-stomatal limitation of photosynthesis. Ramanjulu et al. [46] also found that severe water stress treatment resulted in increased C_i in two mulberry genotypes, while partial stomatal closure at moderate water stress did not cause a decline in C_i in both cultivars, and the non-stomatal limitation of photosynthesis could be calculated by C_i/g_s .

The relative stomatal limitation of photosynthesis, RL_s , can be calculated using the resistance-based method:

$$RL_s = r_s / (r_s + r_a + r^*), \quad (3)$$

where r_s is the stomatal resistance, r_a is the boundary layer resistance, and r^* is the slope of the tangent to the P_n/C_i curve at the operating point.

r_s and r_a can be calculated by:

$$r_s = \frac{1}{g_s}, \quad (4)$$

$$r_a = \frac{n}{0.02} \sqrt{\frac{l_w}{u_h}} \frac{1}{1 - e^{-n/2}}, \quad (5)$$

$$n = \begin{cases} 2.5 & h \ll 1 \\ 2.306 + 0.194h & 1 < h < 10 \\ 4.25 & h \gg 10 \end{cases}, \quad (6)$$

where l_w is the leaf width, u_h is the wind speed at the top of the canopy, and h is the mean height of the canopy.

2.6.2. Decoupling Coefficient and Related Parameters

We calculated Ω according to the method of Jarvis and McNaughton [40]:

$$\Omega = \frac{(\Delta/\gamma + 1)}{(\Delta/\gamma + 1 + g_a/g_c)}, \quad (7)$$

where g_c is the canopy conductance, g_a is the aerodynamic conductance, Δ is the changing rate of saturation vapor pressure with temperature, and γ is the psychrometric constant. The canopy affecting the transpiration of *P. euphratica* is highly coupled with the atmosphere, and *P. euphratica* is well-supplied with water if Ω tends to 0 [47].

The value of g_c is calculated by the inversed Penman–Monteith equation and g_a is obtained according to the method of Granier et al. [48].

$$g_c = \frac{g_a \gamma \lambda T}{\Delta R_n - \lambda T (\Delta + \gamma) + \rho c_p g_a VPD} \times 1000, \quad (8)$$

$$g_a = \frac{k^2 u_h}{\ln[(z - d)/z_0]^2}, \quad (9)$$

where λ is the latent heat of vaporization, ρ is air density, C_p is the specific heat at constant pressure, z is the reference height above the forest at which meteorological measurements are available, d is the zero-plane displacement of a forest with complete canopy cover, z_0 is the roughness length of a forest with complete canopy cover, and k is a constant.

3. Results

3.1. Diurnal Variations in Main Environmental Factors

Detailed information on the key environmental variables is essential to assess diurnal variations in stomatal and non-stomatal limitations of photosynthesis. Average values for environmental factors (PAR, T_a , VPD, and h_s) at the same hour on different observational days in each month were analyzed during the main growing seasons of *P. euphratica* in 2013 and 2014 (Figure 2). Generally, the distribution patterns of PAR, T_a , and VPD all presented single-peak curves. PAR, T_a , and VPD all increased in the morning, peaked between 13:00 and 15:00, and then decreased (Figure 2a–c). During the study periods in both years, the daily average PAR was 941.74 W m^{−2}, varying from 11.62 to 1689.33 W m^{−2}. The daily average T_a was 31.60 °C, which was very near to values obtained for previous years (data not shown). The h_s values decreased gradually after 10:00 (Figure 2d), mainly a result of the increase in T_a , which enhanced evaporation and water loss to the air. The daily average h_s was 46.63%, varying between 17.54% and 75.21%. The values of the four parameters did not show significant differences between 2013 and 2014 (Figure 2).

3.2. Diurnal Variations in the Main Physiological Factors

Physiological factors (P_n , g_s , and C_i) were measured by an LI-6400 portable photosynthesis system on the same days with environmental factors collected from the meteorological station (Figure 3), and the average values of each physiological factor at the same hour on different observational days in each month were analyzed. The distribution patterns of P_n and g_s were similar (Figure 3a,b). P_n increased in the morning, peaked around 14:00, and then decreased. In August and September, the values of P_n were much greater changes than those in June and July (Figure 3a). The g_s values increased rapidly in the morning, peaked between 10:00 and 12:00, and then gradually decreased in the afternoon. The peak values of g_s in different months were reasonably close to one another (0.40–0.46 mol H₂O m^{−2} s^{−1}) (Figure 3b). There were fluctuations in P_n and g_s between 11:00 and 14:00 on several typical sunny days from July to September (Figure 3a,b); C_i presented a contrasting pattern of diurnal changes to P_n and g_s (Figure 3c), with the minimums appearing between 14:00 and 16:00. The ranges of g_s and C_i values in different months were similar, with g_s ranging from 0.02 to 0.47 mol H₂O m^{−2} s^{−1} and C_i ranging from 126.78 to 401.21 μmol CO₂ mol^{−1}.

3.3. Relationships between Environmental Parameters and P_n

Pearson coefficients between environmental parameters and P_n are shown in Table 2. P_n was significantly positively correlated to all of the environmental parameters (PAR, VPD and T_a) except for h_s , and the Pearson coefficients between P_n and PAR were both highest in 2013 (0.820) and 2014 (0.709). Besides the fluctuations in P_n between 11:00 and 14:00 on several typical sunny days, P_n showed the same tendency as PAR in the morning and afternoon (Figures 2a and 3a).

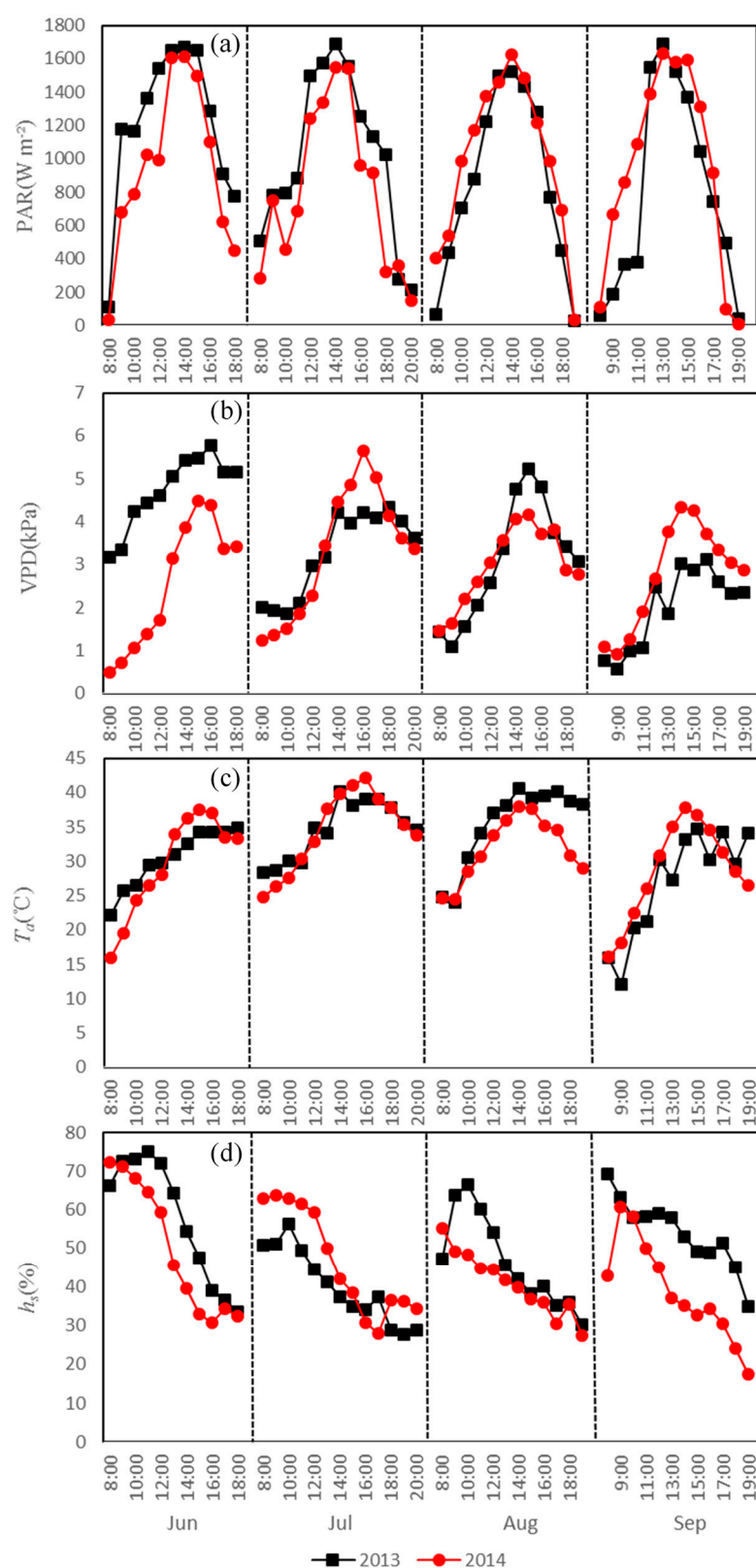


Figure 2. Diurnal variations in (a) photosynthetically active radiation (PAR), (b) vapor pressure deficit (VPD), (c) air temperature (T_a), and (d) relative humidity (h_s) during the main growing seasons of *Populus euphratica* in 2013 and 2014. The values in the figure are the averages for each parameter at the same hour on different observational days in each month.

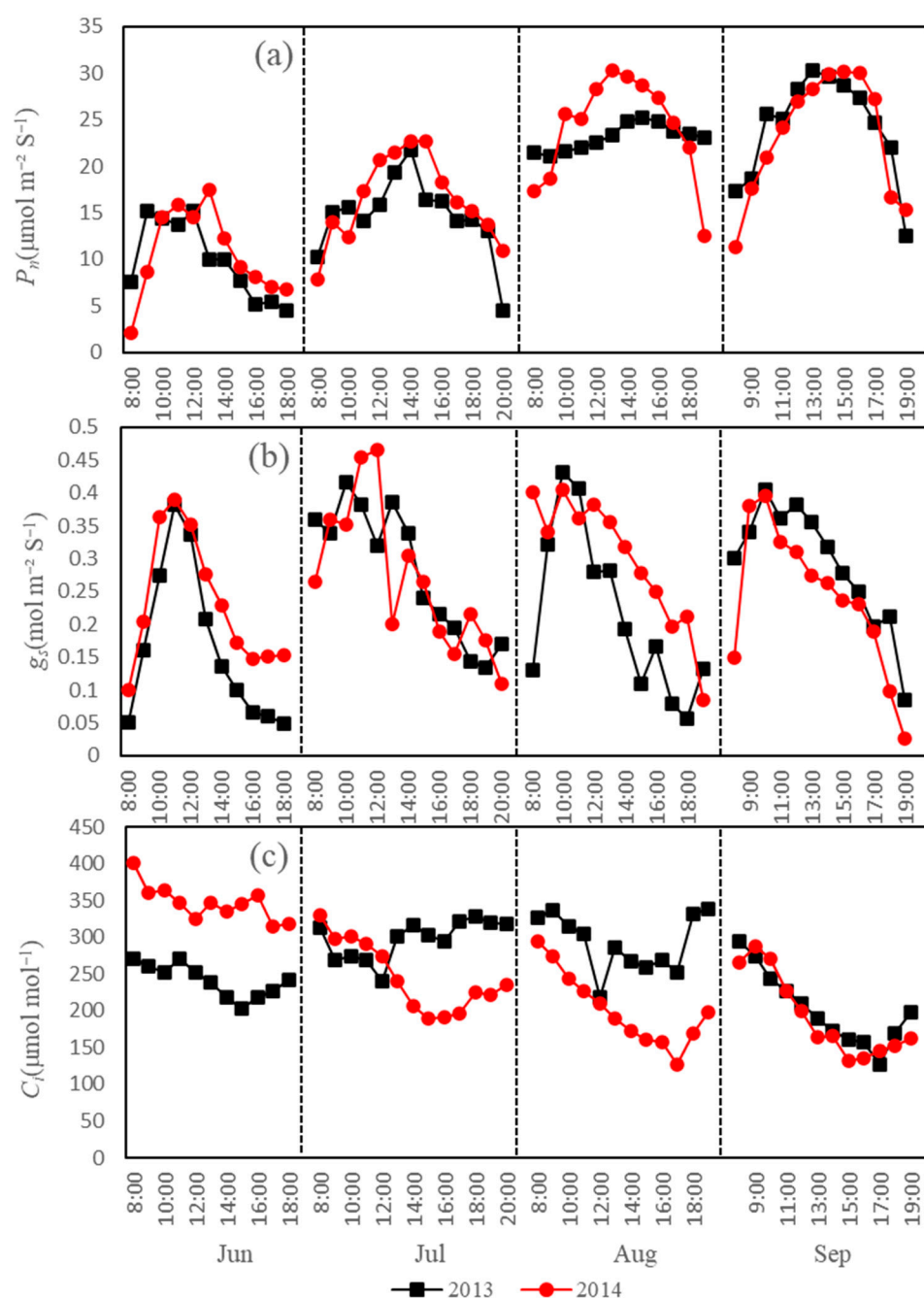


Figure 3. Diurnal variations in (a) net photosynthetic rate (P_n), (b) stomatal conductance (g_s), and (c) intercellular CO_2 concentration (C_i) during the main growing seasons of *Populus euphratica* in 2013 and 2014. The values in the figure are averages for each parameter at the same hour on different observational days in each month.

Table 2. Pearson coefficients between environmental parameters and net photosynthesis (P_n).

	Year	PAR	VPD	T_a	h_s
P_n	2013	0.820 **	0.463 **	0.489 **	−0.180
	2014	0.709 **	0.470 **	0.464 **	−0.370 **

** $p = 0.01$. PAR photosynthetically active radiation, VPD vapor pressure deficit, T_a air temperature, h_s relative humidity.

3.4. Diurnal Variations in Stomatal, Relative Stomatal, and Non-Stomatal Limitations of Photosynthesis

Diurnal variations in L_s , RL_s , and C_i/g_s during the main growing seasons of *P. euphratica* in 2013 and 2014 are shown in Figure 4. Both L_s and RL_s increased in the morning, and then decreased. The L_s values in the afternoon were significantly greater than those in the morning. Generally, the average values of RL_s were greater than those of L_s , while C_i/g_s presented a contrasting pattern of diurnal changes to L_s and RL_s , remaining generally low in the morning and increasing sharply after 17:00. The highest values of these parameters in 2013 and 2014 were 0.70 and 0.51 for L_s , 0.75 and 0.55 for RL_s , and 5.86 and 4.83 for C_i/g_s , respectively.

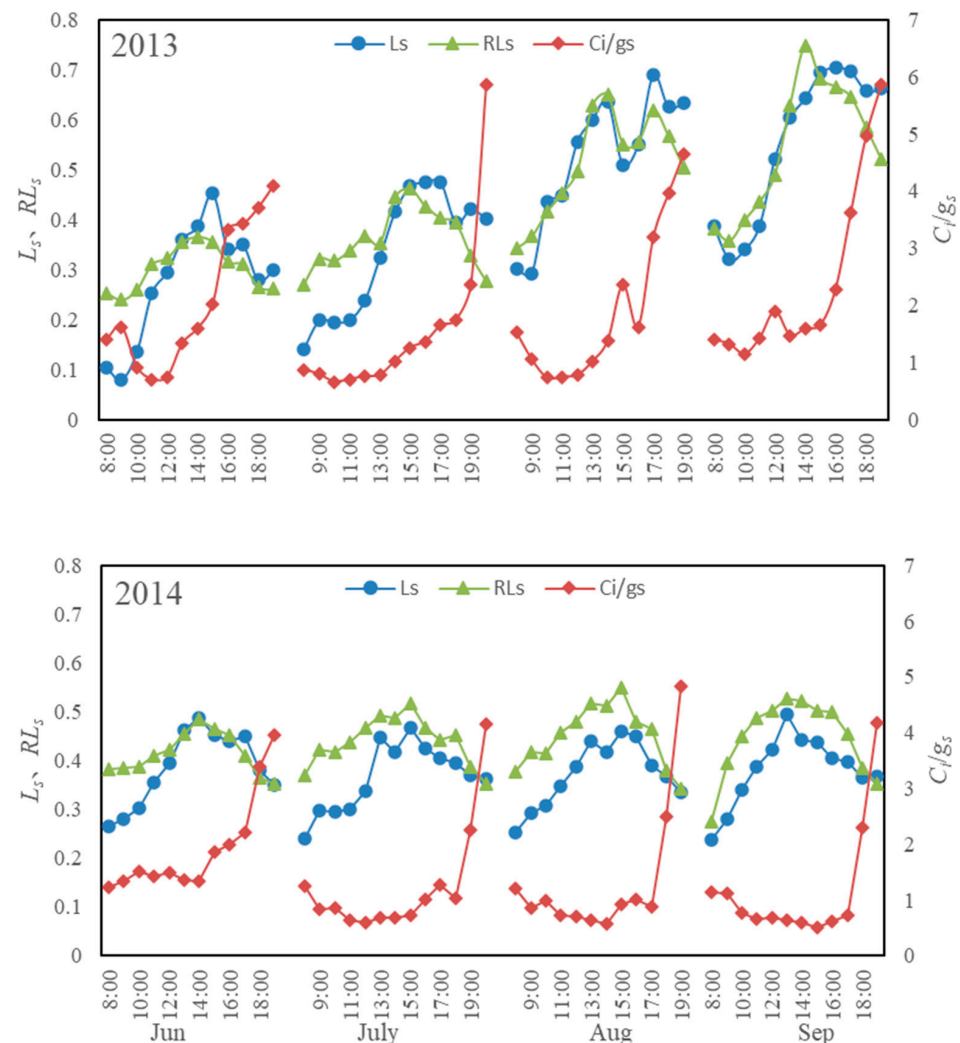


Figure 4. Diurnal variations in the values of stomatal limitation (L_s), relative stomatal limitation (RL_s), and non-stomatal limitation (C_i/g_s) of photosynthesis of *Populus euphratica* leaves during the main growing seasons in 2013 and 2014. The values in the figure are averages for each parameter at the same hour on different observational days in each month.

3.5. Variations in Parameters Related to Water Conditions

We analyzed variations in the parameters indicating water conditions, $-\psi_L$ and Ω (Figures 5 and 6), and the GWT depth (Figure 7), for the *P. euphratica* forest during the main growing season in 2014. Diurnal variations in ψ_L in each month were similar from June to September, decreasing in the morning, reaching a minimum around noon and then increasing. The minimum value of -2.3 MPa occurred in July, and the maximum of nearly -0.2 MPa occurred in the evening in June (Figure 5). The trend of Ω showed a contrasting pattern to ψ_L , with the maximum value occurring at 9:00 or 10:00 and being

slightly greater than 0.1. The Ω values in the afternoon were significantly lower than those in the morning (Figure 6). The depth of the GWT gradually decreased to a minimum (2.22 m) on 18 September, and then increased suddenly to 158 mm above ground following a flood irrigation event that was released from the upper and middle reaches of the Heihe River. After the 10 days of flooding, the depth of the GWT decreased again and fell below the surface water level (Figure 7).

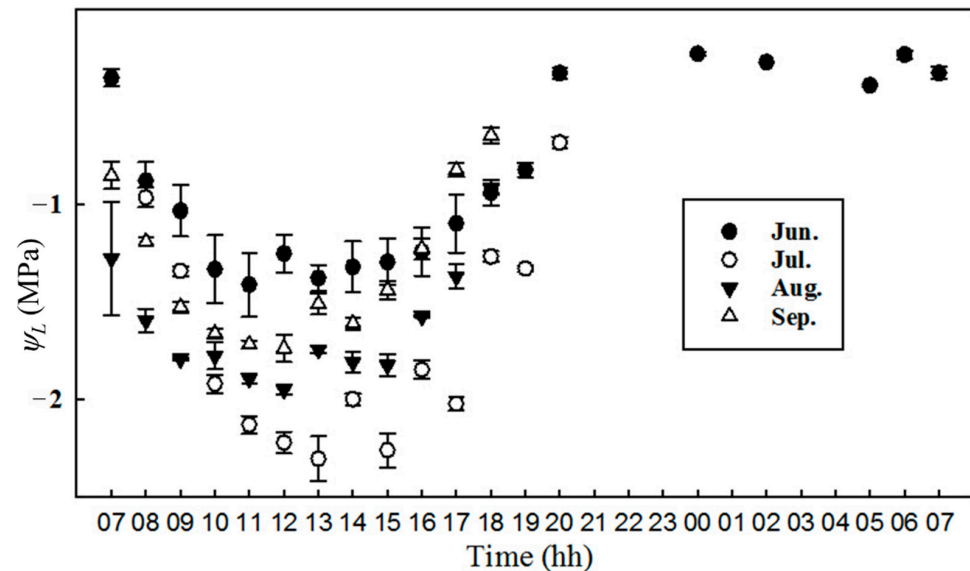


Figure 5. Diurnal variations in leaf water potential (ψ_L) from June to September in 2014. Data were collected over 1 to 2 days of measurements in each month.

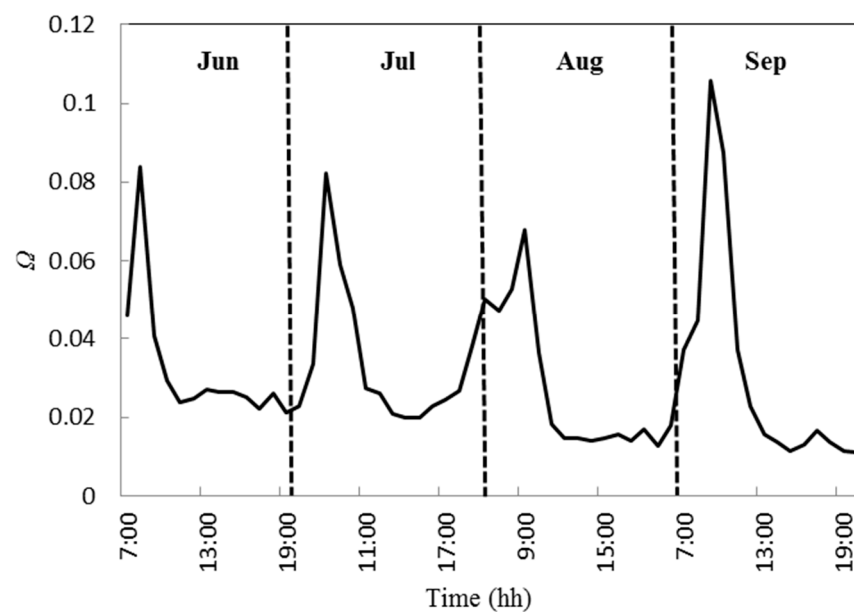


Figure 6. Decoupling coefficient (Ω) for the *Populus euphratica* forest during the growing season in 2014. The values in the figure are averages of Ω at the same hour on different observational days in each month.

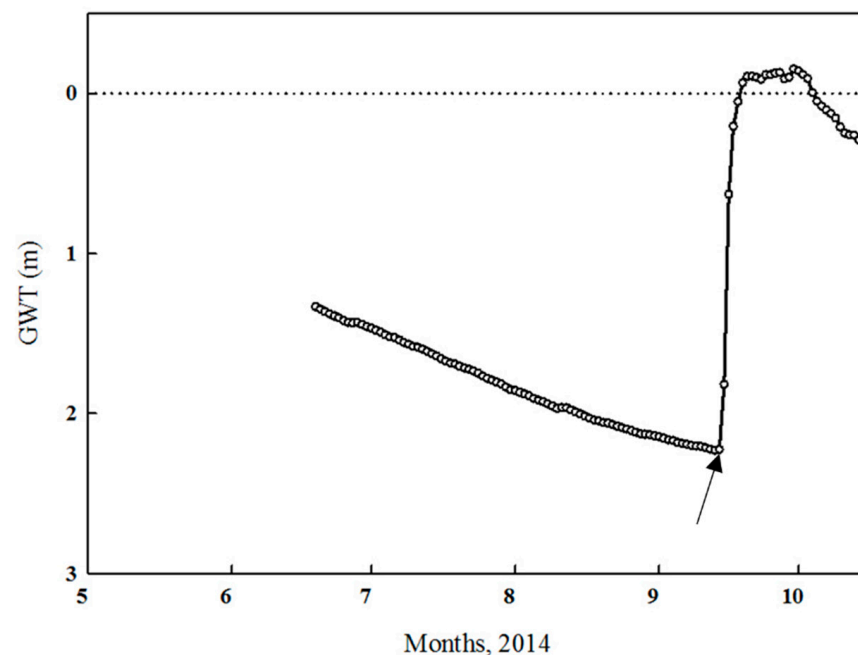


Figure 7. Groundwater table (GWT) for the *Populus euphratica* forest during the growing season in 2014. The arrow indicates the flood irrigation from the upper and middle reaches of the Heihe River detected at our study site after this day.

4. Discussion

4.1. Variations in Physiological Factors and the Phenomenon of Midday Depression of Photosynthesis

Because C_i is a critical physiological factor, the analysis of its variations is indispensable for judging the stomatal and non-stomatal limitations of photosynthesis [49]. In our study, the diurnal variations in C_i presented v-shaped curves (greater C_i values in the morning and evening, and lower values at noon); this is consistent with findings from studies on switchgrass [50] and *Haloxylon ammodendron* [51] in arid regions. The similarity between the distribution patterns of P_n and g_s found in our study (the correlation coefficients were both 0.69 in 2013 and 2014, $p = 0.01^{**}$) and previous studies indicates that g_s is the main factor influencing P_n under extremely arid conditions [52].

During our study periods, we can see a temporary decrease followed by an increase in both P_n and g_s between 11:00 and 14:00 (e.g., July and September in 2013 and July and August in 2014, Figure 3a,b), while PAR increased continually, which indicates the phenomenon of midday depression of photosynthesis (MDP) occurred. This was mainly a result of high transpiration rates caused by high vapor pressure deficit values, which led to an intense leaf water deficit. In turn, the water deficit led to a decrease in g_s and limited the entry of C_a ; this caused a decrease in mesophyll conductance (g_m), which decreased the CO_2 concentration in chloroplasts to a very low level, and reduced P_n . For *P. euphratica* growing in extremely arid regions from July to September, the highest values of T_a and highest transpiration rates occurred near noon. MDP can protect the trees from losing too much water.

4.2. Stomatal, Relative Stomatal, and Non-Stomatal Limitations of Photosynthesis of *P. euphratica*

Although L_s decreased after noon, it remained at a high level and was the main reason for the decrease in P_n in the afternoon. During the MDP periods, L_s peaked and C_i was at a minimum, exhibiting apparent stomatal limitation of photosynthesis. This is consistent with the work of Farquhar and Sharkey [7], who proposed that a simultaneous increase in L_s and decrease in C_i is the criterion for determining stomatal limitation of photosynthesis. The low soil moisture content limited *P. euphratica*'s water uptake, and the intense solar radiation and high VPD values increased the water loss from the trees. Because of the combination of

transpiration and photosynthesis, the stoma closed to maintain the water balance inside the plant and limit the CO_2 entering the leaves. Therefore, stomatal limitation of photosynthesis was predominant. Afterward, L_s decreased and C_i/g_s increased sharply, with non-stomatal limitation of photosynthesis predominating. Other researchers have proposed a variety of criteria for judging stomatal and non-stomatal limitations of photosynthesis; however, these were tested and found to be inappropriate through data and theoretical analysis by Xu [49] (Table 3).

Table 3. Criteria that were tested and found to be inappropriate for judging stomatal and non-stomatal limitations of photosynthesis.

Objectives	Criteria	Source of Data
Stomatal limitation	The decreasing range of C_i is much lower than that of P_n	[53]
Non-stomatal limitation	C_i remains almost constant	[54,55]
Stomatal and non-stomatal limitation	Comparing the values of L_s and C_i/g_s	[56]

Several studies [57–59] have shown that g_m is a main factor controlling the non-stomatal limitation of photosynthesis, especially under stress. The structure of leaves determines the maximum value of g_m [60] that can be achieved, and g_m also changes rapidly according to environmental conditions [61]. In extremely arid regions, where the soil moisture content is very low, water stress is the main factor limiting g_m [62–64]. Because a greater VPD usually leads to lower g_m [65], we can infer that the g_m values in the morning were greater than those in the afternoon, as the VPD changed inversely (Figure 2b). In the morning, it was much easier for C_i to enter the chloroplast through the cytomembrane and cytoplasm, and supply CO_2 for photosynthesis, subsequently leading to low C_i/g_s values. In the afternoon, g_m decreases and restricts the diffusion of CO_2 entering the chloroplast, and subsequently, C_i/g_s increases [51].

Figure 4 shows that the average values of RL_s were greater than those of L_s , mainly as a result of the nonlinearity of the P_n/C_i curve. Such an occurrence often leads to a large overestimation of the importance of the stoma in controlling photosynthesis [8]. Consequently, L_s is more applicable than RL_s for representing the stomatal limitation of photosynthesis.

4.3. Is the Photosynthesis of *P. euphratica* Limited by Drought Stress?

Table 4 summarizes the maximum L_s values of different species from this and previous studies. The maximum L_s values in our study (0.70 in 2013 and 0.51 in 2014) were greater than in others. However, *P. euphratica* was well-supplied with water in our study area, and thus the high values of stomatal limitation of photosynthesis could not be attributed to drought stress, for the following reasons. (1) The minimum ψ_L (−2.3 MPa) was similar to the woody phreatophytes in riparian zones [66,67], and was greater than the hydraulic safety margin (−2.7 MPa) defined by Pan et al. [34]. (2) Previous studies have shown that a GWT depth of less than 4 m is not a limiting factor in the growth of *P. euphratica* [68], as it can grow vigorously with a GWT depth of up to 12 m [66,69]. Hao et al. [70] reported that the GWT depth must be a minimum of 6 m for regular growth of *P. euphratica* in the lower reaches of the Tarim River; this is consistent with the conclusion of Wang et al. [71] regarding the lower Heihe River Basin. The maximum GWT depth in our study was 2.27 m, never exceeding the 6 m threshold. (3) The Ω values in our study were close to 0 (the maximum was slightly greater than 0.1), indicating that the canopy of *P. euphratica* was highly coupled with the atmosphere, and *P. euphratica* was well-supplied with water. This may also explain why g_s remained stable during the growing seasons in 2013 and 2014 (Figure 3b). Additionally, from the initiation of the Ecological Water Diversion Project (2001) to the year before our study (2012), the water flow from Langxin Mountain ranged from 2.04 to 6.99 $\text{m}^3 \text{s}^{-1}$ (Figure 8, data provided by the Heihe River Bureau). These flows

are greater than the lower limit of $1.84 \text{ m}^3 \text{ s}^{-1}$ required to maintain the current scale of Ejn Oasis, as noted by Wang and Cheng [72].

As *P. euphratica* did not experience water stress, we may infer that the stomatal limitation of photosynthesis was likely a result of the conservative water use strategy of *P. euphratica*. Pan et al. [34] and Yu et al. [23] made similar conclusions for the lower reaches of the Tarim and Heihe River, respectively. Additionally, under the high-temperature conditions of the study periods (with mean T_a values at 31.6°C in 2013 and 29.9°C in 2014), the stoma of *P. euphratica* closed to reduce transpiration, resulting in the predominance of stomatal limitation of photosynthesis. Since *P. euphratica* was well-supplied with water, the unsatisfactory recovery of *P. euphratica* is not connected with the water resources. Jiang and Liu [73] concluded that *P. euphratica* simply recovered along the watercourses, while in other areas (especially 1 km from the watercourses), the recovery of *P. euphratica* was not significant. Therefore, optimizing the rational allocation of water resources both along the watercourses and at a distance from them would be a key step for the further recovery of *P. euphratica* in the lower reaches of the Heihe River.

Table 4. Maximum values of stomatal limitation of photosynthesis (L_s) under natural conditions for different species.

Species	Maximum L_s Values	Location	Source of Data
<i>Dacrydium cupressinum</i> Lamb.	0.29	New Zealand	[74]
<i>Metrosideros umbellata</i> Cav.	0.41		
<i>Weinmannia racemosa</i> L.f.	0.42		
<i>Quintinia acutifolia</i> Kirk.	0.41		
<i>Quercus robur</i> L.	0.17	Italy	[57]
<i>Fraxinus oxyphylla</i> Bieb.	0.21	China	[51]
Spring wheat	0.64		
<i>Populus euphratica</i> Oliv.	0.70 (2013) 0.51 (2014)	China	This study

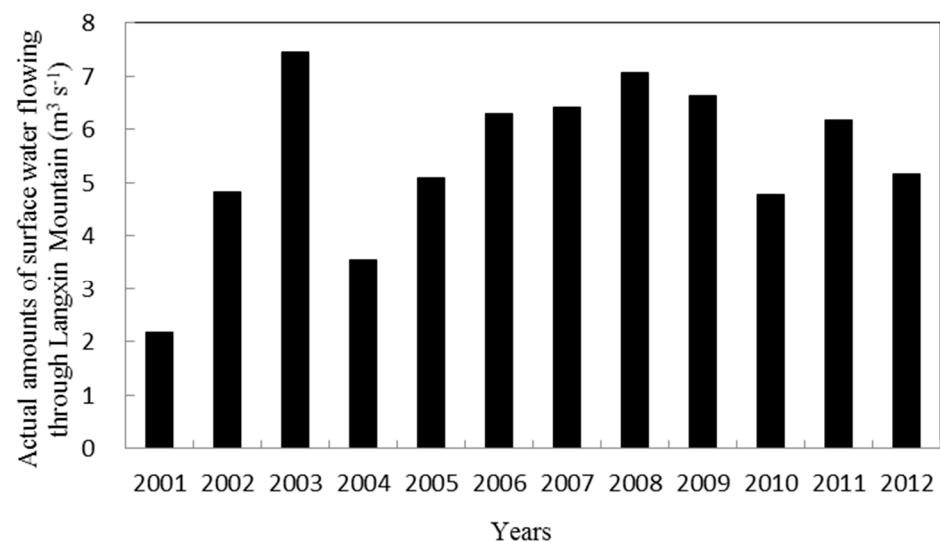


Figure 8. Actual amounts of surface water flowing through Langxin Mountain beginning from the initiation of Ecological Water Diversion Project (2001–2012).

5. Conclusions

We originally attributed the high values of stomatal limitation of photosynthesis to our hypothesis that *P. euphratica* experienced water stress, limiting the photosynthesis processes. However, we concluded that *P. euphratica* was well-supplied with water in our study area based on the analysis of the parameters that indicate water conditions. The stomatal limitation based on photosynthesis values in our study was much greater than that seen in other studies. This can mainly be attributed to the conservative water use strategy of *P. euphratica*, even when growing under favorable water conditions, and extremely high temperatures that induced closure of the stoma to reduce transpiration.

As our data were obtained using the LI-6400 portable photosynthesis system, some parameters were not measured (e.g., chloroplast structure, photosynthetic pigment content, Rubisco activity, RuBP regeneration capacity) to represent the non-stomatal limitation of photosynthesis. Future work will include these parameters.

Author Contributions: Conceptualization, G.G.; methodology, T.Y.; software, X.L.; validation, Q.F. and R.W. All authors have read and agreed to the published version of the manuscript.

Funding: This research was funded by the National Natural Science Foundation of China (U21A20468) and Chinese Post-doctoral Science Foundation (2018M643769).

Acknowledgments: We wish to express our thanks for the support received from the Alax Desert Eco-Hydrology Experimental Research Station, Northwest Institute of Eco-Environment and Resources, Chinese Academy of Sciences. The authors also offer their sincere appreciation for the helpful and constructive comments of the reviewers of the draft manuscript.

Conflicts of Interest: The authors declare no conflict of interest.

References

- Li, D.; Si, J.H.; Zhang, X.Y.; Gao, Y.Y.; Wang, C.L.; Luo, H.; Qin, J.; Gao, G.L. The mechanism of changes in hydraulic properties of *Populus euphratica* in response to drought stress. *Forests* **2019**, *10*, 904. [\[CrossRef\]](#)
- Li, C.Y.; Wang, K.Y. Differences in drought responses of three contrasting *Eucalyptus microtheca* F. Muell. Populations. *For. Ecol. Manag.* **2003**, *179*, 377–385. [\[CrossRef\]](#)
- Zhang, X.; Wu, N.; Li, C. Physiological and growth responses of *Populus davidiana* ecotypes to different soil water contents. *J. Arid Environ.* **2005**, *60*, 567–579. [\[CrossRef\]](#)
- Flexas, J.; Barón, M.; Bota, J.; Ducruet, J.M.; Gallé, A.; Galmés, J.; Jiménez, M.; Pou, A.; Ribas-Carbó, M.; Sajnani, C.; et al. Photosynthesis limitations during water stress acclimation and recovery in the drought-adapted *Vitis* hybrid Richter-110 (*V. berlandieri* × *V. rupestris*). *J. Exp. Bot.* **2009**, *60*, 2361–2377. [\[CrossRef\]](#)
- Makino, A. Photosynthesis, grain yield, and nitrogen utilization in rice and wheat. *Plant Physiol.* **2011**, *155*, 125–129. [\[CrossRef\]](#) [\[PubMed\]](#)
- Munns, R. Comparative physiology of salt and water stress. *Plant Cell Environ.* **2002**, *25*, 239–250. [\[CrossRef\]](#)
- Farquhar, G.D.; Sharkey, T.D. Stomatal conductance and photosynthesis. *Annu. Rev. Plant Physiol.* **1982**, *33*, 317–345. [\[CrossRef\]](#)
- Jones, H.G. Stomatal control of photosynthesis and transpiration. *J. Exp. Bot.* **1998**, *49*, 387–398. [\[CrossRef\]](#)
- Signarbieux, C.; Feller, U. Non-stomatal limitations of photosynthesis in grassland species under artificial drought in the field. *Environ. Exp. Bot.* **2011**, *71*, 192–197. [\[CrossRef\]](#)
- Varone, L.; Ribas-Carbo, M.; Cardona, C.; Gallé, A.; Medrano, H.; Gratani, L.; Flexas, J. Stomatal and non-stomatal limitations to photosynthesis in seedlings and saplings of Mediterranean species pre-conditioned and aged in nurseries: Different response to water stress. *Environ. Exp. Bot.* **2012**, *75*, 235–247. [\[CrossRef\]](#)
- Campos, H.; Trejo, C.; Peña-Valdivia, C.B.; Garcia-Nava, R.; Conde-Martínez, F.V.; Cruz-Ortega, M.R. Stomatal and non-stomatal limitations of bell pepper (*Capsicum annuum* L.) plants under water stress and re-watering: Delayed restoration of photosynthesis during recovery. *Environ. Exp. Bot.* **2014**, *98*, 56–64. [\[CrossRef\]](#)
- Anev, S.; Marinova, A.; Tzvetkova, N.P.; Panayotov, M.P.; Yurukov, S. Stomatal control on photosynthesis in drought-treated subalpine pine saplings. *Genet. Plant Physiol.* **2016**, *6*, 43–53.
- Bastin, J.F.; Berrahmouni, N.; Grainger, A.; Maniatis, D.; Mollicone, D.; Moore, R.; Patriarca, C.; Picard, N.; Sparrow, B.; Abraham, E.M.; et al. The extent of forest in dryland biomes. *Science* **2017**, *356*, 635–638. [\[CrossRef\]](#) [\[PubMed\]](#)
- Reynolds, J.F. Desertification. In *Encyclopedia of Biodiversity*; Levin, S.A., Ed.; Academic Press: San Diego, CA, USA, 2000; pp. 61–78.
- Dai, A. Drought under global warming: A review. *Clim. Chang.* **2011**, *2*, 45–65. [\[CrossRef\]](#)

16. McDowell, N.G.; Coops, N.C.; Beck, P.S.A.; Chambers, J.Q.; Gangodagamage, C.; Hicke, J.A.; Huang, C.Y.; Kennedy, R.; Krofcheck, D.J.; Litvak, M.; et al. Global satellite monitoring of climate induced vegetation disturbances. *Trends Plant Sci.* **2015**, *20*, 114–123. [\[CrossRef\]](#)
17. Sheffield, J.; Wood, E.F.; Roderick, M.L. Little change in global drought over the past 60 years. *Nature* **2012**, *491*, 435–438. [\[CrossRef\]](#)
18. Naithani, K.J.; Ewers, B.E.; Pendall, E. Sap flux-scaled transpiration and stomatal conductance response to soil and atmospheric drought in a semi-arid sagebrush ecosystem. *J. Hydrol.* **2012**, *464–465*, 176–185. [\[CrossRef\]](#)
19. Bhusal, N.; Lee, M.; Han, A.R.; Han, A.; Kim, H.S. Responses to drought stress in *Prunus sargentii* and *Larix kaempferi* seedlings using morphological and physiological parameters. *For. Ecol. Manag.* **2020**, *465*, 118099. [\[CrossRef\]](#)
20. Li, D.; Si, J.H.; Zhang, X.Y.; Gao, Y.Y.; Wang, C.L.; Luo, H.; Qin, J.; Gao, G.L. Hydraulic characteristics of *Populus euphratica* in an arid environment. *Forests* **2019**, *10*, 407. [\[CrossRef\]](#)
21. Si, J.H.; Feng, Q.; Wen, X.H.; Su, Y.H.; Xi, H.Y.; Chang, Z.Q. Major ion chemistry of groundwater in the extreme arid region northwest China. *Environ. Geol.* **2009**, *57*, 1079–1087. [\[CrossRef\]](#)
22. Yu, T.F.; Feng, Q.; Si, J.H.; Pinkard, E.A. Coordination of stomatal control and stem water storage on plant water use in desert riparian trees. *Trees* **2019**, *33*, 787–801. [\[CrossRef\]](#)
23. Yu, T.F.; Feng, Q.; Si, J.H.; Xi, H.Y.; O’Grady, A.P.; Pinkard, E.A. Responses of riparian forests to flood irrigation in the hyper-arid zone of NW China. *Sci. Total Environ.* **2019**, *648*, 1421–1430. [\[CrossRef\]](#) [\[PubMed\]](#)
24. Cheng, G.D.; Li, X.; Zhao, W.Z.; Xu, Z.M.; Feng, Q.; Xiao, S.C.; Xiao, H.L. Integrated study of the water–ecosystem–economy in the Heihe River Basin. *Nat. Sci. Rev.* **2014**, *1*, 413–428. [\[CrossRef\]](#)
25. Zhou, Y.Z.; Li, X.; Yang, K.; Zhou, J. Assessing the impacts of an ecological water diversion project on water consumption through high-resolution estimations of actual evapotranspiration in the downstream regions of the Heihe River Basin, China. *Agric. For. Meteorol.* **2017**, *249*, 210–227. [\[CrossRef\]](#)
26. Guo, Q.L.; Feng, Q.; Li, J.L. Environmental changes after ecological water conveyance in the lower reaches of Heihe River, northwest China. *Environ. Geol.* **2009**, *58*, 1387–1396. [\[CrossRef\]](#)
27. Nian, Y.Y.; Li, X.; Zhou, J. Landscape changes of the Ejin delta in the Heihe River Basin in northwest China from 1930 to 2010. *Int. J. Remote Sens.* **2017**, *38*, 537–557. [\[CrossRef\]](#)
28. Zhang, S.H.; Ye, Z.X.; Chen, Y.N.; Xu, Y.F. Vegetation responses to an ecological water conveyance project in the lower reaches of the Heihe River basin. *Ecolhydrology* **2017**, *10*, e1866. [\[CrossRef\]](#)
29. Chen, Y.P.; Chen, Y.N.; Li, W.H.; Xu, C.C. Characterization of photosynthesis of *Populus euphratica* grown in the arid region. *Photosynthetica* **2006**, *44*, 622–626. [\[CrossRef\]](#)
30. Wang, H.Z.; Han, L.; Xu, Y.L.; Niu, J.L.; Yu, J. Effects of soil water gradient on photosynthetic characteristics and stress resistance of *Populus pruinosa* in the Tarim Basin, China. *Acta Ecol. Sin.* **2017**, *37*, 432–442. (In Chinese) [\[CrossRef\]](#)
31. Zhou, H.H.; Chen, Y.N.; Li, W.H.; Chen, Y.P. Photosynthesis of *Populus euphratica* in relation to groundwater tables and high temperature in arid environment, northwest China. *Photosynthetica* **2010**, *48*, 257–268. [\[CrossRef\]](#)
32. Zheng, C.X.; Qiu, J.; Jiang, C.N.; Yue, N. Comparison of stomatal characteristics and photosynthesis of polymorphic *Populus euphratica* leaves. *Front. For. China* **2007**, *2*, 87–93. [\[CrossRef\]](#)
33. Zhu, G.F.; Li, X.; Su, Y.H.; Lu, L.; Huang, C. Seasonal fluctuations and temperature dependence in photosynthetic parameters and stomatal conductance at the leaf scale of *Populus euphratica* Oliv. *Tree Physiol.* **2011**, *31*, 178–195. [\[CrossRef\]](#) [\[PubMed\]](#)
34. Pan, Y.P.; Chen, Y.P.; Chen, Y.N.; Wang, R.Z.; Ren, Z.G. Impact of groundwater table on leaf hydraulic properties and drought vulnerability of *Populus euphratica* in the Northwest of China. *Trees* **2016**, *30*, 2029–2039. [\[CrossRef\]](#)
35. Chen, Y.N.; Chen, Y.P.; Li, W.H.; Zhang, H.F. Response of the accumulation of proline in the bodies of *Populus euphratica* to the change of groundwater level at the lower reaches of Tarim River. *Chin. Sci. Bull.* **2003**, *48*, 1995–1999. [\[CrossRef\]](#)
36. Kumagai, T.O.; Saitoh, T.M.; Sato, Y.; Morooka, T.; Manfro, O.J.; Kuraji, K.; Suzuki, M. Transpiration, canopy conductance and the decoupling coefficient of a lowland mixed dipterocarp forest in Sarawak, Borneo: Dry spell effects. *J. Hydrol.* **2004**, *287*, 237–251. [\[CrossRef\]](#)
37. Nicolás, E.; Barradas, V.L.; Ortuño, M.F.; Navarro, A.; Torrecillas, A.; Alarcón, J.J. Environmental and stomatal control of transpiration, canopy conductance and decoupling coefficient in young lemon trees under shading net. *Environ. Exp. Bot.* **2008**, *63*, 200–206. [\[CrossRef\]](#)
38. Zhang, Z.Z.; Zhao, P.; McCarthy, H.R.; Zhao, X.H.; Niu, J.F.; Zhu, L.W.; Ni, G.Y.; Ouyang, L.; Huang, Y.Q. Influence of the decoupling degree on the estimation of canopy stomatal conductance for two broadleaf tree species. *Agric. For. Meteorol.* **2016**, *221*, 230–241. [\[CrossRef\]](#)
39. Abdurahman, M.; Kurban, A.; Halik, U.; Ablekim, A.; Duan, H. Study on phenological characters of *Populus euphratica* Oliv. and its relation with the tree diameter. *Vegetos* **2013**, *26*, 88–92. [\[CrossRef\]](#)
40. Jarvis, P.G.; McNaughton, K.G. Stomatal control of transpiration: Scaling up from leaf to region. *Adv. Ecol. Res.* **1986**, *15*, 1–49. [\[CrossRef\]](#)
41. Berry, J.A.; Downton, W.J.S. Environmental regulation of photosynthesis. In *Photosynthesis Vol. II*; Govindjee, N.Y., Ed.; Academic Press: New York, NY, USA, 1982; pp. 263–343.
42. Gao, G.L.; Feng, Q.; Zhang, X.Y.; Si, J.H.; Yu, T.F. An overview of stomatal and non-stomatal limitations to photosynthesis of plants. *Arid. Zone Res.* **2018**, *35*, 929–937. (in Chinese). [\[CrossRef\]](#)

43. Ye, Z.P.; Xie, Z.L.; Duan, S.H.; An, T.; Zeng, G.H.; Kang, H.J. Stomatal and non-stomatal limitations of photosynthesis for *Tetrastigma hemsleyanum* under the condition of facility cultivation. *Plant Physiol. J.* **2020**, *56*, 41–48. (in Chinese). [\[CrossRef\]](#)
44. Song, X.Y.; Zhou, G.S.; He, Q.J.; Zhou, H.L. Stomatal limitations to photosynthesis and their critical water conditions in different growth stages of maize under water stress. *Agr. Water. Manag.* **2020**, *241*, 106330. [\[CrossRef\]](#)
45. Kicheva, M.I.; Tsonev, T.T.; Popova, L.P. Stomatal and nonstomatal limitations to photosynthesis in two wheat cultivars subjected to water stress. *Photosynthetica* **1994**, *30*, 107–116. [\[CrossRef\]](#)
46. Ramanjulu, S.; Sreenivasulu, N.; Sudhakar, C. Effect of water stress on photosynthesis in two mulberry genotypes with different drought tolerance. *Photosynthetica* **1998**, *35*, 279–283. [\[CrossRef\]](#)
47. Burgess, S.S.O.; Adams, M.A.; Turner, N.C.; Beverly, C.R.; Ong, C.K.; Khan, A.A.H.; Bleby, T.M.; Notes, A. An improved heat pulse method to measure low and reverse rates of sap flow in woody plants. *Tree Physiol.* **2001**, *21*, 589–598. [\[CrossRef\]](#)
48. Granier, A.; Loustau, D.; Bréda, N. A generic model of forest canopy conductance dependent on climate, soil water availability and leaf area index. *Ann. For. Sci.* **2000**, *57*, 755–765. [\[CrossRef\]](#)
49. Xu, D.Q. Some problems in stomatal limitation analysis of photosynthesis. *Plant Physiol. Commun.* **1997**, *33*, 241–244. (In Chinese)
50. Gao, Z.J.; Xu, B.C.; Wang, J.; Luo, L.J.; Li, S. Diurnal and seasonal variations in photosynthetic characteristics of switchgrass in semiarid region on the Loess Plateau of China. *Photosynthetica* **2015**, *53*, 489–498. [\[CrossRef\]](#)
51. Yang, Z.S.; Zhang, Q.; Hao, X.C. Stomatal or non-stomatal limitation of photosynthesis of spring wheat flag leaf at late growth stages under natural conditions in semiarid rainfed regions. *Chin. J. Eco-Agric.* **2015**, *23*, 174–182. (In Chinese)
52. Bhusal, N.; Han, S.G.; Yoon, T.M. Impact of drought stress on photosynthetic response, leaf water potential, and stem sap flow in two cultivars of bi-leader apple trees (*Malus × domestica* Borkh.). *Sci. Hortic.* **2019**, *246*, 535–543. [\[CrossRef\]](#)
53. Raschke, K.; Resemann, A. The midday depression of CO₂ assimilation in leaves of *Arbutus unedo* L.: Diurnal changes in photosynthetic capacity related to changes in temperature and humidity. *Planta* **1986**, *168*, 546. [\[CrossRef\]](#) [\[PubMed\]](#)
54. Di Marco, G.; Massacci, A.; Gabrielli, R. Drought effects on photosynthesis and fluorescence in hard wheat cultivars grown in the field. *Physiol. Plant* **1988**, *74*, 385–390. [\[CrossRef\]](#)
55. Tenhunen, J.D.; Lange, O.L.; Gebel, J.; Beyschlag, W.; Weber, J.A. Changes in photosynthetic capacity, carboxylation efficiency, and CO₂ compensation point associated with midday stomatal closure and midday depression of net CO₂ exchange of leaves of *Quercus suber*. *Planta* **1984**, *162*, 193–203. [\[CrossRef\]](#) [\[PubMed\]](#)
56. Guan, Y.X.; Dai, J.Y.; Lin, Y. The photosynthetic stomatal and nonstomatal limitation of plant leaves under water stress. *Plant Physiol. Commun.* **1995**, *31*, 293. (In Chinese)
57. Grassi, G.; Magnani, F. Stomatal, mesophyll conductance and biochemical limitations to photosynthesis as affected by drought and leaf ontogeny in ash and oak trees. *Plant Cell Environ.* **2005**, *28*, 834–849. [\[CrossRef\]](#)
58. Niinemets, Ü.; Cescatti, A.; Rodeghiero, M.; Tosens, T. Complex adjustments of photosynthetic potentials and internal diffusion conductance to current and previous light availabilities and leaf age in Mediterranean evergreen species *Quercus ilex*. *Plant Cell Environ.* **2005**, *29*, 1159–1178. [\[CrossRef\]](#)
59. Warren, C.R. Stand aside stomata, another actor deserves centre stage: The forgotten role of the internal conductance to CO₂ transfer. *J. Exp. Bot.* **2008**, *59*, 1475–1487. [\[CrossRef\]](#)
60. Nobel, P.S. Internal leaf area and cellular CO₂ resistance: Photosynthetic implications of variations with growth conditions and plant species. *Physiol. Plant.* **1977**, *40*, 137–144. [\[CrossRef\]](#)
61. Flexas, J.; Ribas-Carbó, M.; Diaz-Espejo, A.; Galmés, J.; Medrano, H. Mesophyll conductance to CO₂: Current knowledge and future prospects. *Plant Cell Environ.* **2008**, *31*, 602–621. [\[CrossRef\]](#)
62. Scartazza, A.; Lauteri, M.; Guido, M.C.; Brugnoli, E. Carbon isotope discrimination in leaf and stem sugars, water-use efficiency and mesophyll conductance during different developmental stages in rice subjected to drought. *Aust. J. Plant Physiol.* **1998**, *25*, 489–498. [\[CrossRef\]](#)
63. Delfine, S.; Loreto, F.; Alvino, A. Drought-stress effects on physiology, growth and biomass production of rainfed and irrigated bell pepper plants in the Mediterranean region. *J. Am. Soc. Hortic. Sci.* **2001**, *126*, 297–304. [\[CrossRef\]](#)
64. Monti, A.; Brugnoli, E.; Scartazza, A.; Amaducci, M.T. The effect of transient and continuous drought on yield, photosynthesis and carbon isotope discrimination in sugar beet (*Beta vulgaris* L.). *J. Exp. Bot.* **2006**, *57*, 1253–1262. [\[CrossRef\]](#) [\[PubMed\]](#)
65. Bong, G.; Loreto, F. Gas-exchange properties of salt-stressed Olive (*Olea europaea* L.) Leaves. *Plant Physiol.* **1989**, *90*, 1408–1416. [\[CrossRef\]](#) [\[PubMed\]](#)
66. Gries, D.; Zeng, F.J.; Arndt, S.K.; Bruelheide, H.; Thomas, F.M.; Runge, M. Growth and water relations of *Tamarix ramosissima* and *Populus euphratica* on Taklamakan desert dunes in relation to depth to a permanent water table. *Plant Cell Environ.* **2003**, *26*, 725–736. [\[CrossRef\]](#)
67. Zeng, F.; Bleby, T.M.; Landman, P.A.; Adams, M.A.; Arndt, S.K. Water and nutrient dynamics in surface roots and soils are not modified by short-term flooding of phreatophytic plants in a hyperarid desert. *Plant Soil* **2006**, *279*, 129–139. [\[CrossRef\]](#)
68. Li, W.; Zhou, H.; Fu, A.; Chen, Y. Ecological response and hydrological mechanism of desert riparian forest in inland river, northwest of China. *Ecohydrology* **2013**, *6*, 949–955. [\[CrossRef\]](#)
69. Lang, P.; Ahlborn, J.; Schäfer, P.; Wommelsdorf, T.; Jeschke, M.; Zhang, X.M.; Thomas, F.M. Growth and water use of *Populus euphratica* trees and stands with different water supply along the Tarim River, NW China. *For. Ecol. Manag.* **2016**, *380*, 139–148. [\[CrossRef\]](#)

-
70. Hao, X.M.; Li, W.H.; Huang, X.; Zhu, C.G.; Ma, J.X. Assessment of the groundwater threshold of desert riparian forest vegetation along the middle and lower reaches of the Tarim River, China. *Hydrol. Process.* **2010**, *24*, 178–186. [[CrossRef](#)]
 71. Wang, P.; Zhang, Y.; Yu, J.; Fu, G.; Ao, F. Vegetation dynamics induced by groundwater fluctuations in the lower Heihe River Basin, northwestern China. *J. Plant Ecol.* **2011**, *4*, 77–90. [[CrossRef](#)]
 72. Wang, G.X.; Cheng, G.D. Water demand of eco-system and estimate method in arid inland river basins. *J. Desert Res.* **2002**, *22*, 129–134. (In Chinese)
 73. Jiang, X.H.; Liu, C.M. The response of vegetation to water transport in the lower reaches of the Heihe River. *Acta Geogr. Sin.* **2009**, *64*, 791–797. (in Chinese). [[CrossRef](#)]
 74. Tissue, D.T.; Griffin, K.L.; Turnbull, M.H.; Whitehead, D. Stomatal and non-stomatal limitations to photosynthesis in four tree species in a temperate rainforest dominated by *Dacrydium cupressinum* in New Zealand. *Tree Physiol.* **2005**, *25*, 447–456. [[CrossRef](#)] [[PubMed](#)]